NONLINEAR DYNAMICS OF CARBON NANOTUBES

Angelo Oreste Andrisano
Department of Engineering "Enzo Ferrari",
University of Modena and Reggio Emilia, Italy
E-mail: angelooreste.andrisano@unimore.it

Francesco Pellicano
Department of Engineering "Enzo Ferrari",
University of Modena and Reggio Emilia, Italy
E-mail: francesco.pellicano@unimore.it

Matteo Strozzi
Department of Engineering "Enzo Ferrari",
University of Modena and Reggio Emilia, Italy
E-mail: matteo.strozzi@unimore.it

Abstract. *In this paper, the nonlinear vibrations and energy exchange of single-walled carbon nanotubes (SWNTs) are studied. The Sanders-Koiter theory is applied to model the nonlinear dynamics of the system in the case of finite amplitude of vibration. The SWNT deformation is described in terms of longitudinal, circumferential and radial displacement fields. Simply supported, clamped and free boundary conditions are considered. The circumferential flexural modes (CFMs) are investigated. Two different approaches based on numerical and analytical models are compared. In the numerical model, an energy method based on the Lagrange equations is used to reduce the nonlinear partial differential equations of motion to a set of nonlinear ordinary differential equations, which is solved by using the implicit Runge-Kutta numerical method. In the analytical model, a reduced form of the Sanders-Koiter theory assuming small circumferential and tangential shear deformations is used to get the nonlinear ordinary differential equations of motion, which are solved by using the multiple scales analytical method. The transition from energy beating to energy localization in the nonlinear field is studied. The effect of the aspect ratio on the analytical and numerical values of the nonlinear energy localization threshold for different boundary conditions is investigated.*

Keywords*: carbon nanotubes, energy localization, circumferential flexure modes*

1. INTRODUCTION

The spatially localized excitations represent one of the most interesting phenomena in the nonlinear dynamics of solids and structures [1]. In particular, the spatial confinement of nonlinear vibrations generated by external loads can be used to develop robust shock and vibration isolation designs for certain classes of engineering systems [2]. Moreover, excitations of this type determine elementary mechanisms of many physical processes giving noticeable contributions to thermal conductivity [3].

The analogies between the continuous shells and the discrete SWNTs led to a very large application of the elastic shell theories for the SWNT structural analysis. Liew and Wang [4] investigated the wave propagation in SWNTs via two different elastic shell theories, i.e., Love's thin cylindrical shell theory and Cooper-Naghdi thick cylindrical shell theory, the last one taking into account also the shear and inertia effects. Wang et al. [5] studied static buckling and free vibrations of simply supported SWNTs comparing the results of the Donnell shallow shell theory and the simplified Flugge thin shell theory with the results of the exact Flugge thin shell theory, which retains all the three displacement fields. Silvestre [6] investigated the buckling behaviour of clamped SWNTs under external torsion using the Donnell shallow shell theory and the Sanders-Koiter thin shell theory in a wide range of aspect ratios, diameters and chiralities. Strozzi et al. [7] studied the low-frequency linear vibrations of SWNTs in the framework of the Sanders-Koiter thin shell theory. Two approaches, based on numerical and analytical models, were compared. Several types of SWNTs were analysed by varying aspect ratio and chirality.

The effect of the boundary conditions on the nonlinear vibrations of circular cylindrical shells has been deeply investigated in the pertinent literature in the past years. Kurylov and Amabili [8] studied nonlinear vibrations of clamped-free cylindrical shells with geometric imperfection. The Sanders-Koiter shell theory was used to study the nonlinear dynamics. An energy approach based on Lagrange equations was applied to obtain the equations of motion. Pellicano [9] investigated the nonlinear vibrations of cylindrical shells by means of the Sanders-Koiter shell theory. Simply supported and clamped boundary conditions were considered, as well as connections with rigid bodies; in the latter case, experiments were carried out. Zhang et al. [10] used the local adaptive differential quadrature method for the nonlinear vibrations study of simply supported, clamped and free cylindrical shells. The nonlinear equations of motion were formulated by means of the Goldenveizer-Novozhilov shell theory. Strozzi and Pellicano [11] analysed the nonlinear vibrations of functionally graded cylindrical shells for simply supported, clamped and free boundary conditions. The Sanders-Koiter shell theory was applied to describe the nonlinear dynamics of the shell subjected to a harmonic external load.

In the present paper, the nonlinear vibrations and energy exchange of SWNTs are investigated. The SWNT dynamics is studied within the framework of the Sanders-Koiter theory. The circumferential flexural modes (CFMs) are evaluated. The SWNT deformation is described in term of longitudinal, circumferential and radial displacement fields. Simply supported, clamped and free boundary conditions are examined. Two different approaches are proposed, based on numerical and analytical models. In the numerical model, the three displacement fields are expanded in the nonlinear field by using the approximate linear eigenfunctions. An energy method based on the Lagrange equations is used to reduce the nonlinear partial differential equations of motion to a set of nonlinear ordinary differential equations, which is solved by using the implicit Runge-Kutta numerical method. In the analytical model, a reduced form of the Sanders-Koiter shell theory by assuming small circumferential and tangential shear deformations is considered. A fourth-order nonlinear partial differential equation of motion for the radial displacement field is derived, which allows the effect of the nonlinearity for the different boundary conditions to be estimated. An analytical solution of this differential equation of motion is obtained by applying the multiple scales method.

In the second part of the present paper, the transition from energy beating to energy localization in the nonlinear field is investigated; the concept of energy localization is introduced, which represents a strongly nonlinear phenomenon. In the case of small

amplitude initial energy, a periodic energy exchange between the two halves of the nanotube takes place. The nonlinear oscillations of the SWNT become localized when the initial excitation intensity exceeds some energy threshold which depends on the length of the SWNT; the amplitude of the smallest initial excitation, corresponding to the energy confinement in one half of the nanotube axis, is called energy localization threshold.

In this paper, the transition from energy beating to energy localization in SWNTs is investigated using numerical and analytical approaches, where the analytical approach is based on the LPTs concept. The effect of the SWNT aspect ratio on the analytical and numerical values of energy localization threshold is studied; different boundary conditions are evaluated.

2. SANDERS-KOITER NONLINEAR SHELL THEORY

In Figure 1, a circular cylindrical shell having radius R, length L and thickness h is shown; a cylindrical coordinate system (O; x, θ, z) is considered, where the origin O of the reference system is located at the centre of one end of the circular shell. Three displacement fields are represented: longitudinal u (x, θ, t), circumferential v (x, θ, t) and radial w (x, θ, t), where (x, θ) are the longitudinal and angular coordinates, z is the radial coordinate along the thickness h and t is the time.

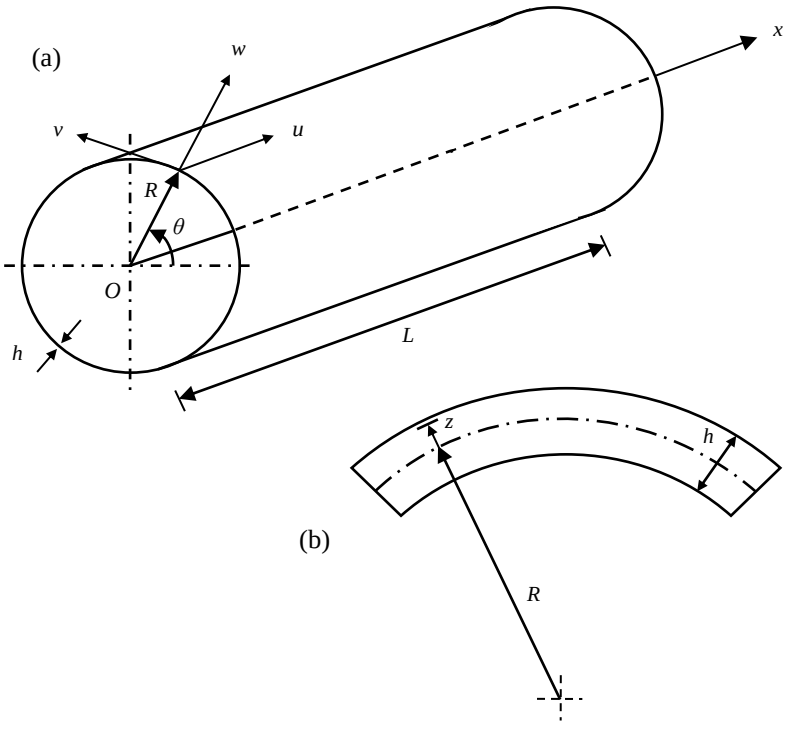

Figure 1. Geometry of the shell. (a) Complete shell; (b) cross-section of the shell surface.

Elastic Strain Energy

The nondimensional elastic strain energy of a circular cylindrical shell is written as [7]

$$\tilde{E} = \frac{1}{2}\frac{1}{(1-\nu^2)}\left[\int_0^1\int_0^{2\pi}\left(\tilde{\varepsilon}_{x,0}^2 + \tilde{\varepsilon}_{\theta,0}^2 + 2\nu\tilde{\varepsilon}_{x,0}\tilde{\varepsilon}_{\theta,0} + \frac{(1-\nu)}{2}\tilde{\gamma}_{x\theta,0}^2\right)d\eta d\theta + \frac{\beta^2}{12}\int_0^1\int_0^{2\pi}\left(\tilde{k}_x^2 + \tilde{k}_\theta^2 + 2\nu\tilde{k}_x\tilde{k}_\theta + \frac{(1-\nu)}{2}\tilde{k}_{x\theta}^2\right)d\eta d\theta\right] \tag{1}$$

where the first term of the right-hand side of equation (1) is the membrane energy (also referred to stretching energy) and the second one is the bending energy, with $\beta = h/R$.

Kinetic Energy

The nondimensional kinetic energy of a circular cylindrical shell is given by [7]

$$\tilde{T} = \frac{1}{2}\gamma\int_0^1\int_0^{2\pi}(\tilde{u}^{\cdot 2} + \tilde{v}^{\cdot 2} + \tilde{w}^{\cdot 2})d\eta d\theta \tag{2}$$

where $\gamma = \rho R^2\omega_0^2 / E$.

3. NUMERICAL SOLUTION OF THE NONLINEAR SHELL THEORY

In order to obtain a numerical solution of the SWNT nonlinear dynamics, a two-steps procedure is considered: i) the three displacement fields are expanded by using the approximated eigenfunctions obtained in linear field; ii) the Lagrange equations are considered in conjunction with the nonlinear elastic strain energy in order to obtain a set of nonlinear ordinary differential equations of motion.

Nonlinear Vibration Analysis

In the nonlinear analysis, the three displacement fields $\tilde{u}(\eta,\theta,\tau)$, $\tilde{v}(\eta,\theta,\tau)$, $\tilde{w}(\eta,\theta,\tau)$ are expanded using the approximated linear mode shapes $\tilde{U}^{(j,n)}(\eta,\theta)$, $\tilde{V}^{(j,n)}(\eta,\theta)$, $\tilde{W}^{(j,n)}(\eta,\theta)$ in the following form [11]

$$\begin{aligned}
\tilde{u}(\eta,\theta,\tau) &= \sum_{j=1}^{N_u}\sum_{n=1}^{N}\tilde{U}^{(j,n)}(\eta,\theta)\,\tilde{f}_{u,j,n}(\tau)\\
\tilde{v}(\eta,\theta,\tau) &= \sum_{j=1}^{N_v}\sum_{n=1}^{N}\tilde{V}^{(j,n)}(\eta,\theta)\,\tilde{f}_{v,j,n}(\tau)\\
\tilde{w}(\eta,\theta,\tau) &= \sum_{j=1}^{N_w}\sum_{n=1}^{N}\tilde{W}^{(j,n)}(\eta,\theta)\,\tilde{f}_{w,j,n}(\tau)
\end{aligned} \tag{3}$$

where the time laws $(\tilde{f}_{u,j,n}(\tau), \tilde{f}_{v,j,n}(\tau), \tilde{f}_{w,j,n}(\tau))$ are unknown functions (step i).

Lagrange Equations

Expansions (3) are inserted into the expressions of elastic strain energy $\tilde{E}$ (1) and kinetic energy $\tilde{T}$ (2); then, the nondimensional Lagrange equations of motion for free vibrations can be expressed in the form [11]

$$\frac{d}{d\tau}\left(\frac{\partial \tilde{T}}{\partial \dot{\tilde{q}}_i}\right)+\frac{\partial \tilde{E}}{\partial \tilde{q}_i}=0 \qquad i\in[1,N_{\max}] \tag{4}$$

where the maximum number of degrees of freedom $N_{\max}$ depends on the number of vibration modes considered in the expansions (3).

By using the Lagrange equations (4), a set of nonlinear ordinary differential equations of motion is obtained (step ii), which is solved numerically using the implicit Runge-Kutta method with suitable accuracy, precision and number of steps.

4. ANALYTICAL SOLUTION OF THE NONLINEAR SHELL THEORY

In order to obtain an analytical solution of the SWNT nonlinear dynamics, a two-steps procedure is considered: i) a reduced form of the Sanders-Koiter nonlinear theory is developed, and a nonlinear partial differential equation of motion is obtained for the radial displacement field; ii) the Galerkin method is considered in order to obtain a set of nonlinear ordinary differential equations of motion.

Nonlinear Vibration Analysis

The nonlinear expansions of the nondimensional longitudinal $\tilde{u}$, circumferential $\tilde{v}$ and radial $\tilde{w}$ displacement fields can be written as [7]

$$\begin{aligned}\tilde{u}(\eta,\theta,\tau)&=\tilde{U}_0(\eta,\tau)+\tilde{U}(\eta,\tau)\cos(n\theta)\\ \tilde{v}(\eta,\theta,\tau)&=\tilde{V}(\eta,\tau)\sin(n\theta)\\ \tilde{w}(\eta,\theta,\tau)&=\tilde{W}_0(\eta,\tau)+\tilde{W}(\eta,\tau)\cos(n\theta)\end{aligned} \tag{5}$$

where $\tilde{U}_0$ and $\tilde{W}_0$ are the axisymmetric component of longitudinal and radial displacements.

By neglecting the nondimensional middle surface circumferential normal strain [7]

$$\tilde{\varepsilon}_{\theta,0}=\frac{\partial \tilde{v}}{\partial \theta}+\tilde{w}+\frac{1}{2}\left(\frac{\partial \tilde{w}}{\partial \theta}-\tilde{v}\right)^2+\frac{1}{8}\left(\frac{\partial \tilde{u}}{\partial \theta}-\alpha\frac{\partial \tilde{v}}{\partial \eta}\right)^2=0 \tag{6}$$

and the nondimensional middle surface tangential shear strain [7]

$$\tilde{\gamma}_{x\theta,0}=\frac{\partial \tilde{u}}{\partial \theta}+\alpha\frac{\partial \tilde{v}}{\partial \eta}+\alpha\frac{\partial \tilde{w}}{\partial \eta}\left(\frac{\partial \tilde{w}}{\partial \theta}-\tilde{v}\right)=0 \tag{7}$$

the nondimensional longitudinal and circumferential displacement fields can be written as functions of the nondimensional radial displacement field.

The nonlinear partial differential equation of motion for the nondimensional radial displacement field is written in the following form (step i) [7]

$$\frac{\partial^2\tilde{W}}{\partial\tau^2}+\frac{\beta^2n^2(n^2-1)^2}{12(n^2+1)}\tilde{W}-\frac{\alpha^2\beta^2(n^2-1)(n^2-1+\nu)}{6(n^2+1)}\frac{\partial^2\tilde{W}}{\partial\eta^2}-\frac{\alpha^2}{n^2(n^2+1)}\frac{\partial^4\tilde{W}}{\partial\eta^2\partial\tau^2}+$$
$$\frac{\alpha^4(12+n^4\beta^2)}{12n^2(n^2+1)}\frac{\partial^4\tilde{W}}{\partial\eta^4}+\frac{(n^2-1)^4}{2n^2(n^2+1)}\tilde{W}\left[\left(\frac{\partial\tilde{W}}{\partial\tau}\right)^2+\tilde{W}\frac{\partial^2\tilde{W}}{\partial\tau^2}\right]+\frac{2\alpha^4(n^2-1)^2}{n^2(n^2+1)}\left(\frac{\partial\tilde{W}}{\partial\tau}\right)^2$$
$$\frac{\partial^2\tilde{W}}{\partial\eta^2}+\frac{\alpha^2(n^2-1)^2}{2n^2(n^2+1)}\left[2\frac{\partial\tilde{W}}{\partial\tau}\frac{\partial\tilde{W}}{\partial\eta}\frac{\partial^2\tilde{W}}{\partial\eta\partial\tau}-\tilde{W}\left(\frac{\partial^2\tilde{W}}{\partial\eta\partial\tau}\right)^2+\left(\frac{\partial\tilde{W}}{\partial\tau}\right)^2\frac{\partial^2\tilde{W}}{\partial\eta^2}\right]+\frac{\alpha^4}{2n^2(n^2+1)} \tag{8}$$
$$\left[\frac{\partial^2\tilde{W}}{\partial\eta\partial\tau}\left(\frac{\partial^2\tilde{W}}{\partial\eta\partial\tau}\frac{\partial^2\tilde{W}}{\partial\eta^2}+2\frac{\partial\tilde{W}}{\partial\eta}\frac{\partial^3\tilde{W}}{\partial\eta^2\partial\tau}\right)+\frac{\partial\tilde{W}}{\partial\eta}\left(\frac{\partial\tilde{W}}{\partial\eta}\frac{\partial^4\tilde{W}}{\partial\eta^2\partial\tau^2}+2\frac{\partial^3\tilde{W}}{\partial\eta\partial\tau^2}\frac{\partial^2\tilde{W}}{\partial\eta^2}\right)\right]=0$$

Galerkin Procedure

Assuming that the solution of the nonlinear equation (8) under simply supported boundary conditions is represented as follows (discretization method) [7]

$$\tilde{W}(\eta,\tau)=\tilde{f}_1(\tau)\sin(\pi\eta)+\tilde{f}_2(\tau)\sin(2\pi\eta) \tag{9}$$

we can get a set of two nonlinear ordinary differential modal equations of motion for the two modal amplitudes $\tilde{f}_1, \tilde{f}_2$ by using the Galerkin method (step ii).

This system of two nonlinear equations of motion is solved analytically by applying the asymptotic expansion and the multiple scales method.

5. NUMERICAL RESULTS

In this section, the analytical and numerical values of the nonlinear energy localization threshold are compared; different aspect ratios of the SWNT are evaluated; the influence of the boundary conditions is investigated.

The mechanical parameters of the SWNT analysed in this paper are shown in Table 1; comparisons between the natural frequencies of the SWNT of Table 1 obtained by using the previous analytical and numerical methods for the circumferential flexural modes are reported in Ref. [7].

Table 1. Mechanical parameters of the SWNT.

Young's modulus *E*	5.5 TPa
Poisson's ratio *ν*	0.19
Mass density *ρ*	11700 kg/m^3
Thickness *h*	0.066 nm
Radius *R*	0.786 nm

Energy Localization Threshold

In this section, the analytical and numerical estimations of the nonlinear energy localization threshold are compared for different boundary conditions; the comparisons are carried out in the interval of the aspect ratios $\lambda = 20 \div 90$.

In the case of simply supported boundary conditions (Figure 2 and Table 2), the results of the analytical and numerical methods are very close for the whole interval of the aspect ratios. A fast increment of the localization threshold in the lower region of the aspect ratios $\lambda = 20 \div 40$ is found; the localization threshold increment is monotonic with L/R, reaching an horizontal asymptote at $\lambda \approx 70$.

In the case of clamped-clamped boundary conditions (Figure 3 and Table 3), the results of the analytical and numerical methods are close for the whole interval of the aspect ratios. The localization threshold increases with L/R up to $\lambda = 35$, where the frequency ratios $\omega_{3,2}/\omega_{1,2}$ and $\omega_{2,2}/\omega_{1,2}$ approach the unity ($\lambda = 30$: $\omega_{2,2}/\omega_{1,2} = 1.032$, $\omega_{3,2}/\omega_{1,2} = 1.118$; $\lambda = 40$: $\omega_{2,2}/\omega_{1,2} = 1.012$, $\omega_{3,2}/\omega_{1,2} = 1.044$) and a 1:1:1 weak internal resonance takes place. Then, there is a localization threshold decrement up to $\lambda = 40$, which is followed by a maximum of localization threshold at $\lambda \approx 50$, where the frequency ratios $\omega_{3,2}/\omega_{2,2}$ and $\omega_{2,2}/\omega_{1,2}$ approach the unity ($\lambda = 45$: $\omega_{2,2}/\omega_{1,2} = 1.009$, $\omega_{3,2}/\omega_{2,2} = 1.021$; $\lambda = 55$: $\omega_{2,2}/\omega_{1,2} = 1.004$, $\omega_{3,2}/\omega_{2,2} = 1.008$) and a 1:1:1 strong internal resonance takes place. The localization threshold decreases with L/R from $\lambda = 55$, achieving an horizontal asymptote at $\lambda \approx 80$.

In the case of free-free boundary conditions (Figure 4 and Table 4), the results of the analytical and numerical methods are close for the whole interval of the aspect ratios. A very slow increment of the localization threshold in the lower region of the aspect ratios $\lambda = 20 \div 50$ is found. A jump of the localization threshold is located at $\lambda = 55$, where the frequency ratios $\omega_{3,2}/\omega_{2,2}$ and $\omega_{2,2}/\omega_{1,2}$ approach the unity ($\lambda = 50$: $\omega_{2,2}/\omega_{1,2} = 1.0015$, $\omega_{3,2}/\omega_{2,2} = 1.0061$; $\lambda = 60$: $\omega_{2,2}/\omega_{1,2} = 1.0010$, $\omega_{3,2}/\omega_{2,2} = 1.0036$) and a 1:1:1 strong internal resonance takes place. The localization threshold increment is then monotonic with L/R.

For all the boundary conditions, the results of the analytical and numerical methods are in perfect agreement for $\lambda \geq 70$, since the effect of the boundary conditions can be neglected far from the edges.

6. CONCLUSIONS

In this paper, the nonlinear vibrations and energy exchange of SWNTs are studied. The Sanders-Koiter theory is applied to model the nonlinear dynamics of the system. Simply supported, clamped and free boundary conditions are considered. The CFMs are analysed. Two different approaches are developed, where the nonlinear partial differential equations of motion are solved considering numerical (implicit Runge-Kutta) and analytical (multiple scales) methods.

The influence of the aspect ratio on the analytical and numerical values of the energy localization threshold is investigated in nonlinear field. For all the considered boundary conditions, the results of the analytical and numerical methods almost coincide at the high aspect ratios, since the boundary conditions effect can be neglected far from the edges.

Moreover, a good correspondence between the results of the two approaches is found for the intermediate interval of the aspect ratios, where a maximum of the localization threshold in the case of clamped edges and a jump of the localization threshold in the case of free edges take place, which are related to internal resonances.

The present paper, which is devoted to the CFMs, could represent a framework also in the study of the nonlinear vibrations and energy exchange of the beam-like modes (BLMs) and the radial breathing (axisymmetric) modes (RBMs).

Table 2. Amplitude of the localization threshold. Simply supported SWNT of Table 1. Different aspect ratios L/R. Comparisons between analytical and numerical results.

Aspect ratio L/R	Analytical method	Numerical method	Difference %
20	0.14283	0.14593	2.17
25	0.15902	0.16123	1.39
30	0.16608	0.16739	0.79
35	0.16917	0.17001	0.50
40	0.17058	0.17112	0.31
45	0.17124	0.17172	0.28
50	0.17155	0.17201	0.27
55	0.17169	0.17213	0.26
60	0.17175	0.17217	0.25
65	0.17176	0.17218	0.24
70	0.17175	0.17216	0.24
75	0.17173	0.17213	0.23
80	0.17171	0.17211	0.23
85	0.17168	0.17207	0.23
90	0.17166	0.17204	0.22

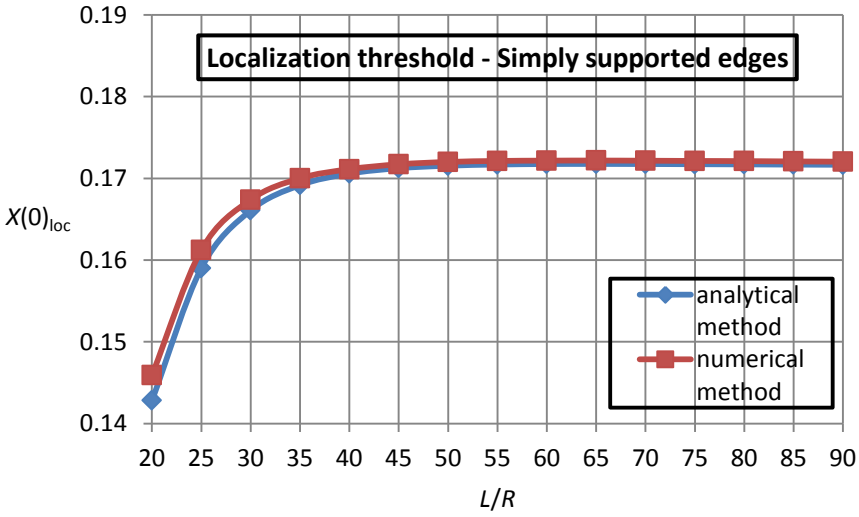

Figure 2. Effect of the aspect ratio on the amplitude of localization threshold for the simply supported SWNT of Table 1. "-♦-", analytical method; "-■-", numerical method.

Table 3. Amplitude of the localization threshold. Clamped-clamped SWNT of Table 1. Different aspect ratios L/R. Comparisons between analytical and numerical results.

Aspect ratio L/R	Analytical method	Numerical method	Difference %
20	0.16623	0.17020	2.39
25	0.16740	0.17118	2.26
30	0.17240	0.17616	2.18
35	**0.17975**	**0.18298**	**1.80**
40	0.17267	0.17528	1.51
45	0.19043	0.19279	1.24
50	**0.57890**	**0.58486**	**1.03**
55	0.26399	0.26613	0.81
60	0.21539	0.21685	0.68
65	0.19652	0.19762	0.56
70	0.18512	0.18595	0.45
75	0.18040	0.18112	0.40
80	0.17790	0.17854	0.36
85	0.17639	0.17699	0.34
90	0.17542	0.17600	0.33

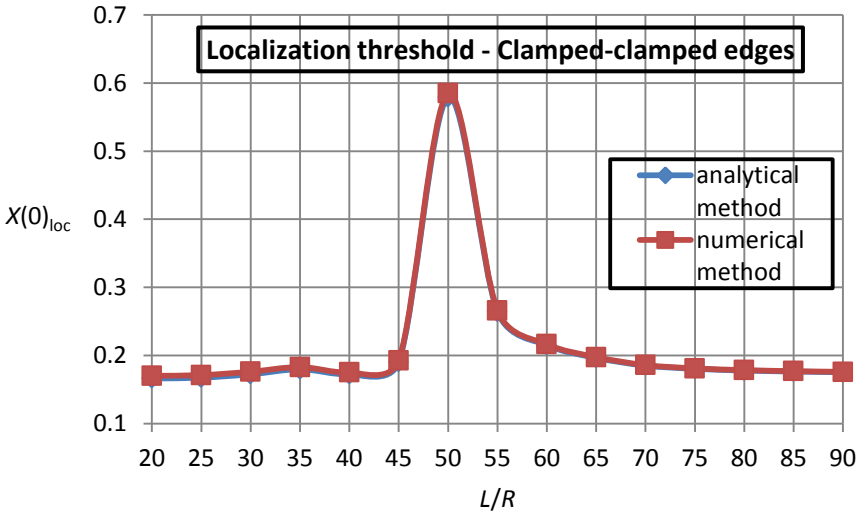

Figure 3. Effect of the aspect ratio on the amplitude of localization threshold for the clamped-clamped SWNT of Table 1. "-♦-", analytical method; "-■-", numerical method.

Table 4. Amplitude of the localization threshold. Free-free SWNT of Table 1. Different aspect ratios L/R. Comparisons between analytical and numerical results.

Aspect ratio L/R	Analytical method	Numerical method	Difference %
20	0.06790	0.07048	3.80
25	0.07267	0.07521	3.49
30	0.07770	0.08022	3.24
35	0.08230	0.08432	2.46
40	0.08625	0.08788	1.89
45	0.08959	0.09093	1.50
50	0.09223	0.09332	1.18
55	**0.13008**	**0.13125**	**0.90**
60	0.13351	0.13442	0.68
65	0.13643	0.13718	0.55
70	0.13893	0.13958	0.47
75	0.14110	0.14172	0.44
80	0.14301	0.14361	0.42
85	0.14466	0.14524	0.40
90	0.14613	0.14670	0.39

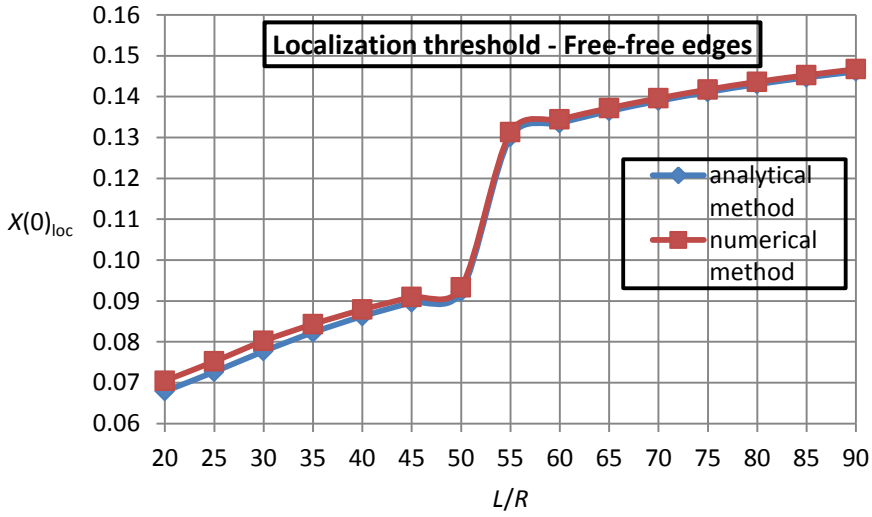

Figure 4. Effect of the aspect ratio on the amplitude of localization threshold for the free-free SWNT of Table 1. "-♦-", analytical method; "-■-", numerical method.

REFERENCES

[1] Manevitch LI, Gendelman OV, 2011. *Tractable Models of Solid Mechanics. Formulation, Analysis and Interpretation*.

[2] Balandin DV, Bolotnik NN, and Pilkey WD, 2001. *Optimal Protection From Impact, Shock, and Vibration*.

[3] Scott A, 2003. *Nonlinear Science: Emergence and Dynamics of Coherent Structures*.

[4] Liew KM, Wang Q, 2007. "Analysis of wave propagation in carbon nanotubes via elastic shell theories", *International Journal of Engineering Science*, **45**, pp. 227-241.

[5] Wang CY, Ru CQ, and Mioduchowski A, 2004. "Applicability and Limitations of Simplified Elastic Shell Equations for Carbon Nanotubes", *Journal of Applied Mechanics*, **71**, pp. 622-631.

[6] Silvestre N, 2012. "On the accuracy of shell models for torsional buckling of carbon nanotubes", *European Journal of Mechanics A/Solids*, **32**, pp. 103-108.

[7] Strozzi M, Manevitch LI, Pellicano F, Smirnov VV, and Shepelev DS, 2014. "Low-frequency linear vibrations of single-walled carbon nanotubes: Analytical and numerical models", *Journal of Sound and Vibration*, **333**, pp. 2936-2957.

[8] Kurylov Y, Amabili M, 2011. "Nonlinear vibrations of clamped-free circular cylindrical shells", *Journal of Sound and Vibration*, **330**, pp. 5363-5381.

[9] Pellicano F, 2007. "Vibrations of circular cylindrical shells: Theory and experiments", *Journal of Sound and Vibration*, **303**, pp. 154-170.

[10] Zhang L, Xiang Y, and Wei G, 2006. "Local adaptive differential quadrature for free vibration analysis of cylindrical shells with various boundary conditions", *International Journal of Mechanical Sciences*, **48**, pp. 1126-1138.

[11] Strozzi M, Pellicano F, 2013. "Nonlinear vibrations of functionally graded cylindrical shells", *Thin-Walled Structures*, **67**, pp. 63-77.